ENVIRONMENTAL RESEARCH
LETTERS

LETTER • OPEN ACCESS

Satellite observations reveal stable forest limits and shrub expansion across the Canadian forest-tundra ecotone

To cite this article: H Travers-Smith *et al* 2025 *Environ. Res. Lett.* **20** 104006

ENVIRONMENTAL RESEARCH
LETTERS

CrossMark

OPEN ACCESS

RECEIVED
21 May 2025

REVISED
23 July 2025

ACCEPTED FOR PUBLICATION
18 August 2025

PUBLISHED
2 September 2025

LETTER

Satellite observations reveal stable forest limits and shrub expansion across the Canadian forest-tundra ecotone

H Travers-Smith[1,*], N C Coops[1], C Mulverhill[1], M A Wulder[2], T C Lantz[3] and D D Ignace[4]

1 Department of Forest Resource Management, University of British Columbia, Vancouver, BC V6T 1Z4, Canada
2 Canadian Forest Service, (Pacific Forestry Centre), Natural Resources Canada, Victoria, BC V8Z 1M5, Canada
3 School of Environmental Studies, University of Victoria, Victoria, BC V8W 2Y2, Canada
4 Department of Forest Resources, University of Minnesota, St. Paul, MN 55108, United States of America
* Author to whom any correspondence should be addressed.

E-mail: hanats@student.ubc.ca

Keywords: vegetation structure, forest-tundra, treeline, Landsat, ICESat-2, climate change

Supplementary material for this article is available online

Abstract

Climate change at high latitudes is expected to increase the cover of woody vegetation across the forest-tundra ecotone. However, there is still uncertainty concerning the nature and magnitude of these changes. In this study, we used open access satellite remote sensing data from ICESat-2 and Landsat to model change in vegetation structure across 183 million hectares of the Canadian forest-tundra ecotone from 1985 to 2021. We used Random Forests models to predict canopy presence and height across six time periods at 30 m spatial resolution. Change between time periods was used to classify nine stable and transitional vegetation types. We used these data to map advance and retreat in the northernmost forest limit and linked change types to disturbance history. Over the study period, the extent of forested area increased by 0.9% and the forest limit warmed by 1.08 °C, receiving 25 mm more annual precipitation. However, large parts of the forest limit remained stable over time despite favorable climate conditions. Our mapping also revealed divergent patterns in forest and shrub expansion across the ecotone, with shrubs exhibiting more widespread and diffuse expansion above the forest limit. Increasing vegetation structure across the ecotone was strongly associated with fire history as 80% of mapped vegetation changes occurred in disturbed areas. The majority of forest growth and new forest expansion occurred in fires that burned over 40 years ago. These findings highlight the importance of disturbance-recovery dynamics in structural vegetation change over decadal time periods.

1. Introduction

High latitudes are experiencing rapid climate shifts, and vegetation is responding to change in growing season length, temperature, precipitation and fire regimes (Matasci *et al* 2018, Berner *et al* 2020, Myers-Smith *et al* 2020, Orndahl *et al* 2022). The forest-tundra ecotone (FTE), located between the boreal and tundra biomes is expected to be a catalyst for future vegetation change (Payette *et al* 2001, Berner and Goetz 2021). Projected increases in temperature and precipitation could facilitate northward advance of the boreal biome over the next century (Pearson *et al* 2013, Montesano *et al* 2024). These changes are concerning due to broad-scale implications for habitat quality and availability (Rickbeil *et al* 2018, Speed *et al* 2021), carbon storage (Epstein *et al* 2012), and permafrost stability (Chapin *et al* 2000).

Over recent decades, boreal forests have shown mixed response to climate change. Satellite observations of tree cover suggest that losses due to fires below the treeline are greater than forest expansion at the treeline (Rotbarth *et al* 2023). This is consistent with fine-scale observations showing limited change (Evans and Brown 2017, Brodie *et al* 2019, Rotbarth *et al* 2023), or no northward advance of latitudinal treelines despite favorable climate conditions (Lantz *et al* 2019, Timoney *et al* 2019, Timoney and Mamet 2020, Maher *et al* 2021). Vegetation change in the FTE is complex and changes in forest cover are also influenced by expansion of tall shrubs (Brodie *et al* 2019, Terskaia *et al* 2020). Shrubs have shown more rapid responses to climate compared to conifers (Travers-Smith and Lantz 2020), and establishment of tall shrubs may restrict future tree establishment in the tundra (Terskaia *et al* 2020). Taken together, these findings indicate complex relationships between climate and potential shifts in the boreal biome, in part due to interactions with fire and shrub expansion.

To date, remote sensing studies of northern vegetation have largely focused on analyzing patterns in spectral greening indices, including the Normalized Difference Vegetation Index and the Enhanced Vegetation Index (EVI; Guay *et al* 2014, Sulla-Menashe *et al* 2018, Berner *et al* 2020, Myers-Smith *et al* 2020, Berner and Goetz 2021, Chen *et al* 2021). Spectral greening trends have been associated with increasing Leaf Area Index (Myers-Smith *et al* 2011, McManus *et al* 2012), vegetation phytomass (Walker *et al* 2003, Epstein *et al* 2012), and growing season length (Arndt *et al* 2019). Stronger greening trends at the northern margin of the boreal have been speculated to indicate northward advance of the biome (Sulla-Menashe *et al* 2018, Berner and Goetz 2021). However, greenness indices alone are not always strong predictors of forest structure due to confounding signals from the ground and understory vegetation (Loranty *et al* 2018, Walker *et al* 2021). Indices that incorporate longer wavelengths, including shortwave infrared, may be better predictors of forest cover and canopy height at the treeline (Fraser *et al* 2017, Travers-Smith *et al* 2025). Thus, linking spectral indices to the physical characteristics of vegetation may improve remotely sensed indicators of forest change (Rotbarth *et al* 2023).

Active remote sensing such as Light Detection and Ranging (lidar) provides direct measurements of vegetation height and cover that can be integrated with spectral time-series to map vegetation structure over large areas (Matasci *et al* 2018, Mulverhill *et al* 2022, Montesano *et al* 2024). Current models of structural change in the FTE are limited due to the high cost of lidar acquisitions in the north (Margolis *et al* 2015). Spaceborne lidar platforms can help address limitations with cost and scale, collecting standardized height measurements across the globe. Currently, ICESat-2 is the only spaceborne lidar platform operating above 51° latitude (Markus *et al* 2017). ICESat-2 was launched in 2018 and carries a single-photon counting lidar system with three pairs of green (532 nm) lasers that illuminate the ground every 70 cm along the satellite's path (Magruder *et al* 2021). Geolocated photon returns are classified into and summary statistics of canopy and terrain height are calculated within 20 m and 100 m segments (Neuenschwander and Pitts 2019). Canopy height measurements from ICESat-2 have been validated across boreal forests (Neuenschwander *et al* 2020, Mulverhill *et al* 2022, Feng *et al* 2023) and used to derive wall-to-wall mapping products in various ecosystems (Shah *et al* 2020, Sothe *et al* 2022, Malambo *et al* 2023, Travers-Smith *et al* 2024).

To better inform future projections of change in the forest-tundra ecotone, multi-decadal monitoring is needed to capture gradual ecological processes, including northward forest advance (Timoney 2023). In this study, we use lidar measurements from ICESat-2, and Landsat time-series to model vegetation change across 183 million hectares of the Canadian FTE. We examine long-term trends in vegetation presence and height over 36 years and classify multiple types of structural change at 30 m spatial resolution. These data were used to address the following research questions: (1) Are observed changes in forested area consistent with climate-driven northward advance of the forest limit? (2) How has vegetation cover and height changed across the Canadian FTE? And (3) How much of these changes are attributable to disturbance-recovery dynamics?

2. Methods

2.1. Study area

Our study area encompasses 183 million hectares of the Canadian FTE within Yukon Territory, Northwest Territories, Nunavut, northern Quebec and the Newfoundland-Labrador peninsula (figure 1). This region traverses the traditional territories of many Indigenous peoples including the Dene, Inuit, Cree and Métis peoples. In particular, a significant portion of the FTE is within Inuit Nunangat—the Inuit homeland which includes the Inuvialuit, Nunavut, Nunavik and Nunatsiavut regions (RCGS 2018a). The Denendeh and Eeyou Istchee regions encompass large areas of northern boreal forest below of the treeline, and are home to many Dene and Cree communities (RCGS 2018b).

Climate, vegetation, and soils vary across the study area and are controlled by latitude, proximity to the ocean and glacial history (Ecosystem Classification Group 2007, 2012). Climate is cold with mean annual temperatures below freezing (Wang *et al* 2016). Between 1948 and 2018 air temperatures warmed by approximately 1 °C–3 °C, with more rapid warming in the northwest (Vincent *et al* 2020). Precipitation has also increased at a rate of 1.5%–2% per decade, with a greater proportion falling as rain (Box *et al* 2019).

The Taiga Plains, Taiga Shield and Southern Arctic ecozones make up the majority of the study area. The Taiga Plains are located in the northwest part of the study area and white spruce (*Picea glauca*) and black spruce (*Picea mariana*) are the dominant species at the treeline (Timoney *et al* 1992). The boundary between the Taiga Plains in the west

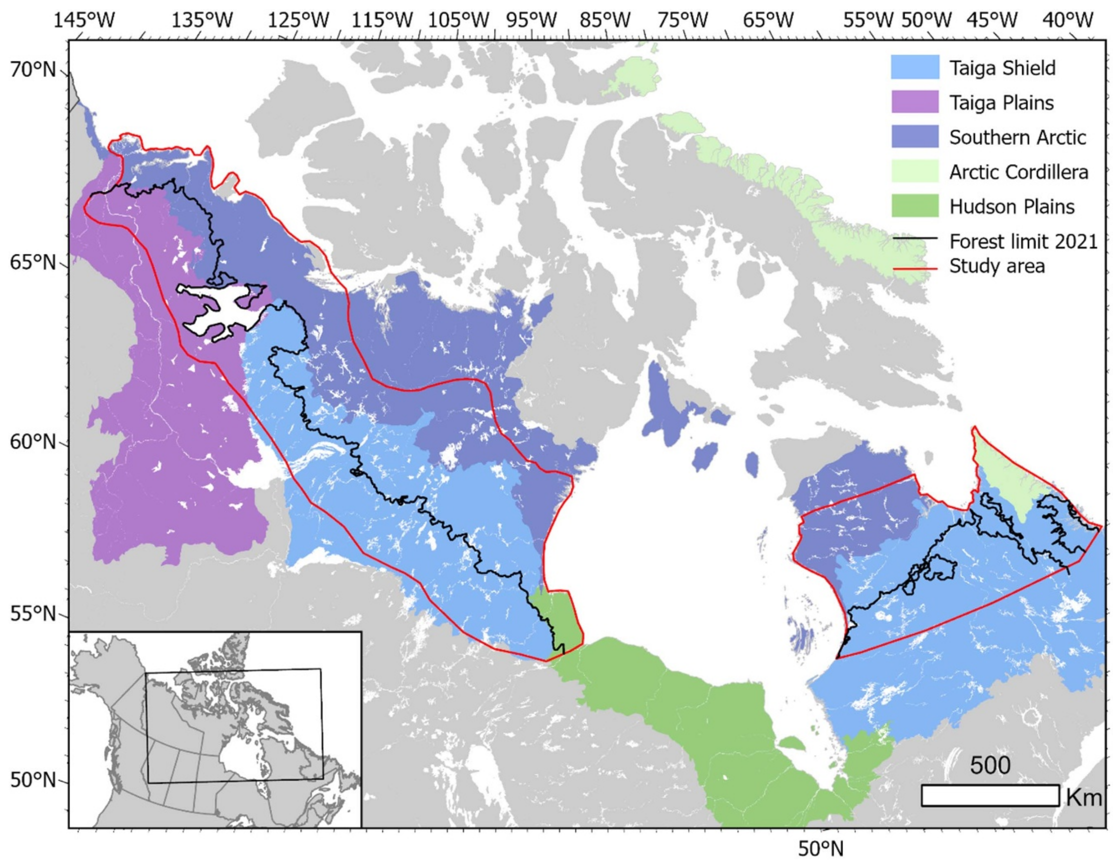

Figure 1. Map of the Canadian arctic and sub-arctic. The red outline indicates the extent of the forest-tundra ecotone study area. The shaded areas, defined in the legend, show the extent of the major ecoregions in the study area and the solid black line indicates the extent of the continuous 3 m forest limit (Travers-Smith *et al* 2024).

and the Taiga Shield in the east is defined by the extent of Precambrian granite that is characteristic of the Shield (Ecosystem Classification Group 2008). The width of the ecotone increases across the Taiga Shield and drops southward in latitude (Timoney *et al* 1992). Soils in this region are relatively nutrient poor with areas of exposed bedrock supporting black spruce (*Picea mariana*) and Jack pine (*Pinus banksiana*) at the treeline (Timoney *et al* 2019). The Southern Arctic makes up the northernmost part of the study area and is largely treeless hosting extensive lake and stream networks (Ecosystem Classification Group 2012).

2.2. Data

2.2.1. IceSat-2

We used the ICESat-2 Land and Vegetation Height ATL08 product (version 5) to sample canopy presence and vegetation height. We followed previously published procedures to extract high quality ATL08 20 m segments suitable for spatial modelling (Mulverhill *et al* 2022, Travers-Smith *et al* 2024). Segments were filtered based on the quality control flags to remove samples impacted by water, blowing snow, aerosols, multiple scattering effects and clouds. The terrain quality flag was also used to remove segments where the estimated ground height was outside of an acceptable range from a reference Digital Terrain Model (DTM). To broadly correspond with the 30 m resolution of Landsat and ASTER-GDEM data, we used 98th percentile canopy height within 20 m segments. To align ATL08 segments with spectral and topographic covariates, we created a 20 m buffer around the center of each ATL08 segment and joined the canopy height attributes to the mean pixel values of each layer intersecting with the buffer. In total, we used 982 296 ATL08 segments from the strong beams acquired in the months of December and January from 2019 to 2021.

2.2.2. Landsat Best Available Pixel (BAP)

Landsat BAP composites use multiple images across a single growing season to generate annual cloud and gap free mosaics of surface reflectance (White *et al* 2014). The radiometric stability of surface reflectance data can vary across bands and sensors (Mishra *et al* 2016, Sulla-Menashe *et al* 2016). When selecting pixels for inclusion in a given BAP composite, priority is given to pixels closest to the center of the annual growing season (1 August) that are free of atmospheric interference from clouds, shadow or haze. Missing reflectance values are imputed using temporal trends fit across the entire time series (Hermosilla *et al* 2015). This surface reflectance product provides consistency over time and space, and has been used as the foundation for a range of time-series analysis conducted over Canada's forested ecoregions (Hermosilla *et al* 2018, 2025, Matasci *et al* 2018). We expect Landsat surface reflectance values to represent similar physical features over time, which supports modeling both current and historic vegetation conditions (Hermosilla *et al* 2018).

We used annual composites to generate spectral predictor variables over the following six decadal time periods: 1985–1995, 1990–2000, 1995–2005, 2000–2010, 2005–2015, 2010–2021. Overlapping 10 year time periods were chosen due to the stronger predictive power of long-term average reflectance values in Random Forests models (Bolton *et al* 2018). Additionally, annual BAP composites earlier in the time-series have more missing values that have been temporally filled (Hermosilla *et al* 2015). Longer time periods (>5 years) ensure there are adequate number of real surface reflectance measurements in each period. In each time period, we derived the median spectral value across six spectral bands (red, green, blue, NIR, SWIR1, SWIR2) and derived four multi-band indices: tasseled cap brightness (TCB), tasseled cap wetness, tasseled cap greenness (TCG) and the EVI using equations from Hermosilla *et al* (2022). Pixels experiencing a stand replacing disturbance during the time series were identified using the Composite2Change data product and removed from model training (Hermosilla *et al* 2016). To remove pixels impacted by drainage and expansion of waterbodies, we generated a mask of maximum water extent using minimum thresholds in annual TCB and EVI and removed pixels with water in three or more years of the time series.

2.2.3. ASTER-GDEM

The ASTER Global Digital Elevation Map (Tachikawa *et al* 2011; version 2) was used to derive four topographic predictors at 30 m spatial resolution: elevation, slope, aspect and Topographic Position Index (TPI). Slope, aspect and TPI were calculated from the DEM using the adjacent eight pixels in R using the terrain function in the 'raster' package (Hijmans 2022). TPI was calculated as the difference in elevation between a pixel and the mean of its neighbors.

2.2.4. Northwest territories fire history

Within a subset of our study area, we used a dataset of fire boundaries that burned between 1950 and 2020 across the Northwest Territories to examine associations between vegetation change and fire history (NWT Centre for Geomatics 2024). This dataset represents one of the most comprehensive records of fire history in northern Canada and uses historic air photographs to map fires that burned before the satellite record. Fires were grouped into the following classes: undisturbed, pre-1985, 1985–1999 and 2000–2011.

2.3. Random forests modeling

In each time period ($n = 6$), we used a Random Forests classification model to predict the probability of canopy presence or absence (%), and a Random Forests regression model to predict canopy height (m), following a similar workflow described in Travers-Smith *et al* (2024). Additional validation of modeled canopy height using independent airborne lidar data is also reported in Travers-Smith *et al* (2024). Models were trained using the ten spectral variables from the last decadal time period (2010–2021) corresponding with the 2019–2021 ICESat-2 ATL08 acquisitions ($n = 982\,396$), and the four topographic variables from the ASTER-GDEM data. We created a dataset to train the models using ATL08 segments representing undisturbed and spectrally homogenous areas within a 20 m circular buffer around the center of each ATL08 segment. Within the buffer we extracted the coefficient of variation in spectral values and disturbance history. Segments with no disturbance history over the Landsat record and a coefficient of variation <10% were selected for model training ($n = 565\,541$). After training, models were tested on all remaining segments not used in the training datasets. The models and predictions were generated using the 'ranger' *R* package (Wright and Ziegler 2017). We used the unscaled permutation method to assess relative variable importance, which calculates the increase in MSE when the values of each predictor variable are randomly permuted.

The canopy presence model was trained on 300 000 ATL08 segments labeled as 'canopy present' or 'canopy absent'. The labels were based on the land cover flag in the ATL08 metadata and a minimum number of four number photons classified as 'canopy' or 'top of canopy' in each 20 m segment (Travers-Smith *et al* 2024). The probability of canopy presence and absence (ranging from 0%–100%), represents the proportion of decision trees in the forest that predicted each class. The number of trees was set to 1001 (to break ties) and the *mtry* parameter set to five. The canopy height regression model was trained on 193 805 segments, representing all of the undisturbed and spectrally homogenous segments with a canopy present. The Random Forests regression model was generated using 1000 trees and the *mtry* parameter was seven. We also assigned a weight to each sample (*case_weights*) to increase the probability of sampling high and low canopy heights. This helps mitigate the effect of sample averaging within decision trees that reduces the range of the predicted values relative to the training data. Weights were defined based on the number of standard deviations away from the mean, with greater weight assigned to samples further from the mean. To assess how spectral indices in our model capture variation in vegetation structure, we sampled 200 000 pixels classified as no canopy, 1–3 m 3–5 m, 5–10 m and >10 m and plotted the distribution of spectral values and indices within each structural class.

2.4. Mapping advance of the northern forest limit

We used the canopy presence and canopy height layers to map the northernmost extent of vegetation at least 3 m in height for the first and last decadal periods in the analysis (1985–1995, 2010–2021). The difference between these extents was used to evaluate northward advance of the boreal forest. We used a 3 m threshold because this limit aligns best with the forest-tundra boundary defined by Timoney *et al* (1992). This threshold also represents a general boundary between tall shrubs and low-stature forests close to the treeline, while still being detectable in spaceborne lidar data (Travers-Smith *et al* 2024). Thus, change in the 3 m forest limit is likely to represent advance or retreat of a meaningful, ecological boundary. In both time periods, canopy height was set to 0 m when the probability of canopy presence was <50%. We summarized mean canopy height within a 1 × 1 km grid and classified cells using a 3 m threshold in mean canopy height. From the classified grid, we created polygons representing forested and non-forested areas and generated a smoothed continuous boundary generalizing the geometry of the resulting features. To quantify areas representing advance and retreat of the forest limit, we calculated the difference between the extent of continuous 3 m forest area in 1995 and 2021 and removed regions covered by water bodies. An advance in the forest limit indicates the region within the 2021 forest boundary that was not in the 1995 forest boundary. Retreat indicates regions within the 1995 forest boundary that was not in the 2021 forest boundary. To evaluate climatic constraints on northward forest advance, we used interpolated climate data at 1 km spatial resolution from ClimateNA (Wang *et al* 2016) to extract mean annual temperature and total annual precipitation for pixels intersecting the forest limit for both time periods.

2.5. Defining vegetation structural change classes

We used a heuristic model to classify 30 m pixels into nine stable and transitional vegetation classes (table 1). Within each time period ($n = 6$) we classified pixels into three structural types: no canopy, shrub (1–3 m) or forest (>3 m). Next, we compared the majority class between the first and last three time periods. If the majority was the same, the pixel was classified as 'stable no canopy', 'stable shrub' or 'stable forest', according to the majority class over time. The following transitional vegetation types were defined based on change in the majority vegetation class: 'canopy loss' (forest or shrub to no canopy), 'new shrub' (no canopy to shrub), 'new forest' (no canopy or shrub to forest), 'shrub infilling' (forest to shrub). For pixels with majority forest class, we calculated linear trends in canopy height to further identify 'forest growth' (increasing height) and 'shrub infilling' (decreasing height). We plotted the distribution of t-scores across the study area (supplemental figure 1) and used a threshold of ±1.69 to capture non-trended, increasing and decreasing trends in forest height. Due to the greater uncertainty in heights below 3 m we did not calculate linear trends in height within the shrub class. Finally, if a pixel transitioned from the forest to shrub class or vice versa, but there was no significant trend in height we classified it as 'stable low forest'. This accounts for potential spurious transitions between the forest and shrub class in pixels that are close to the 3 m threshold.

Table 1. Descriptions of the nine structural vegetation types classified at 30 m spatial resolution. Decision rules were based on change in the majority class between the first and last three time periods and linear trends in canopy height.

Vegetation class	Decision rules
Stable no canopy	Majority no canopy class
Stable shrub (1–3 m)	Majority shrub class
Stable forest (>3 m)	Majority forest class & no trend in height
Stable low forest	Change between forest and shrub classes but no trend in height
Forest growth	Majority forest class & increasing height
Shrub infilling	Forest to shrub change OR majority forest with decreasing height
Canopy loss	Change from forest or shrub to no canopy
New forest	Change from no canopy or shrub to forest
New shrub	Change from no canopy to shrub

3. Results

3.1. Model performance & spectral indicators of vegetation structure

The Random Forests canopy presence model had an overall 89.9% accuracy on the test dataset ($n = 682\,396$). Canopy presence was detected with 82% accuracy while canopy absence was detected with 93% accuracy. The regression model predicting canopy height had overall RMSE was 1.93 m and R^2 was 0.47 on the test dataset ($n = 154\,287$). In both classification and regression models, topographic predictors had low variable importance compared to the spectral bands and indices. The most important variables in the classification model were the SWIR1 and red bands and TCB. Similarly for the height model the most important variables were TCB and the NIR and SWIR2 bands. Overall, shortwave infrared reflectance and the TCB index decreased within increasing vegetation structure figure 2. Near-infrared reflectance and TCG showed non-linear relationships with structure. Spectral greenness was greatest in the 1–3 m height

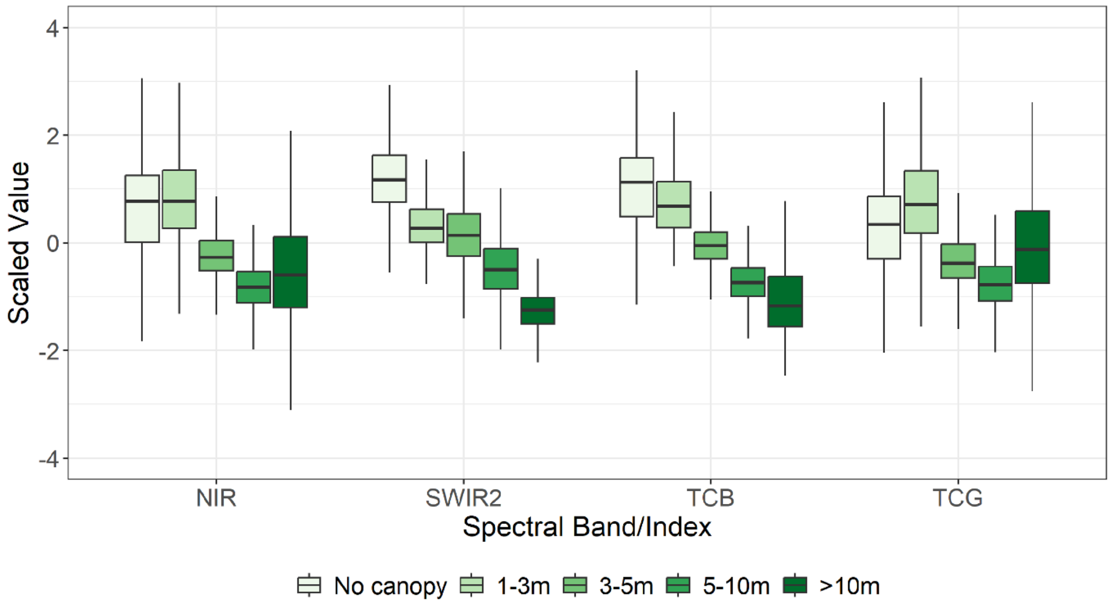

Figure 2. Variation in spectral predictors (Band 4: NIR, Band 8: SWIR 2, Tasseled Cap Brightness Index and Tasseled Cap Greenness Index), that were important in the Random Forests models among canopy height classes. Note that the data were scaled for plotting on the same *y*-axis and values show the number of standard deviations away from the mean value for each band or index.

range and intermediate canopy heights (3–10 m) showed the lowest greenness values (figure 2).

3.2. Change in the forest limit

Overall, the extent of continuous 3 m forest was similar between the two time periods (1985–1995 and 2010–2021; figure 3). The area of 3 m forest increased by 15 921 km^2 (0.9% of the 1995 forest extent). The area representing forest advance was 24 146 km^2 and the area representing retreat was 8,225 km^2. Advance was not uniform across the study area, and large parts of the 1995 forest limit were unchanged in 2021 (figure 2). Areas of advance were spatially constrained and tended to occur between neighboring areas of the forest limit. The Taiga Shield east of Hudson's Bay showed more advance than western Canada, with 12 264 km^2 of new continuous forest area. The Taiga Shield and the Hudson Plains ecozone west of Hudson's Bay showed the most extensive forest retreat (figure 3). Analysis of climate variables along the forest limit show that mean annual temperature at the forest limit has warmed by 1.08 °C and total annual precipitation increased by 25 mm from 1985 to 2021.

3.3. Structural vegetation change

The vast majority of the study area had stable vegetation structure over time (92%), with 45% classified as 'no canopy', 34% as 'forest' and 9% as 'shrub' (figure 4 and table 2). The Southern Arctic showed the least amount of change with 2.3% classified as transitional, while 11.7% and 10.7% of the Taiga Plains and Taiga Shield showed structural change, respectively (table 2). The most frequently occurring type of change was 'shrub infilling' covering 3.2% of the study area (table 2). The 'forest growth' class covered 1.8% of the study area and 'canopy loss' covered 1.2% of the study area. Both the 'new forest' and 'new shrub' classes showed similar coverage with 0.7%–0.9% respectively (table 2).

Maps showing the distribution of the transitional classes indicate divergent patterns in forest and shrub expansion across the ecotone (figure 5). Pixels classified as 'new forest' are generally close to or below the historic forest limit, while 'new shrub' pixels show widespread and diffuse presence above the forest limit (figure 5). The northwestern part of the study area shows concentrated 'forest growth' compared to Nunavik on the eastern side of Hudson's Bay, which shows a greater amount of 'shrub infilling' (figure 5). The central part of the study area also has a higher concentration of canopy loss, likely associated with fires.

Fire history accounts for a high proportion of structural change, with 80% of transitional pixels located in fire boundaries. Older fires that burned before 1985 were more likely to show increasing forest structure with 17.3% and 6.1% of these areas classified as 'forest growth' or 'new forest', respectively (table 3). In undisturbed areas, 'forest growth' and 'new forest' covered 1.9% and 0.4%, respectively. As expected, recent fires had a higher proportion of pixels classified as 'shrub infilling' and 'canopy loss' compared to undisturbed areas (table 3).

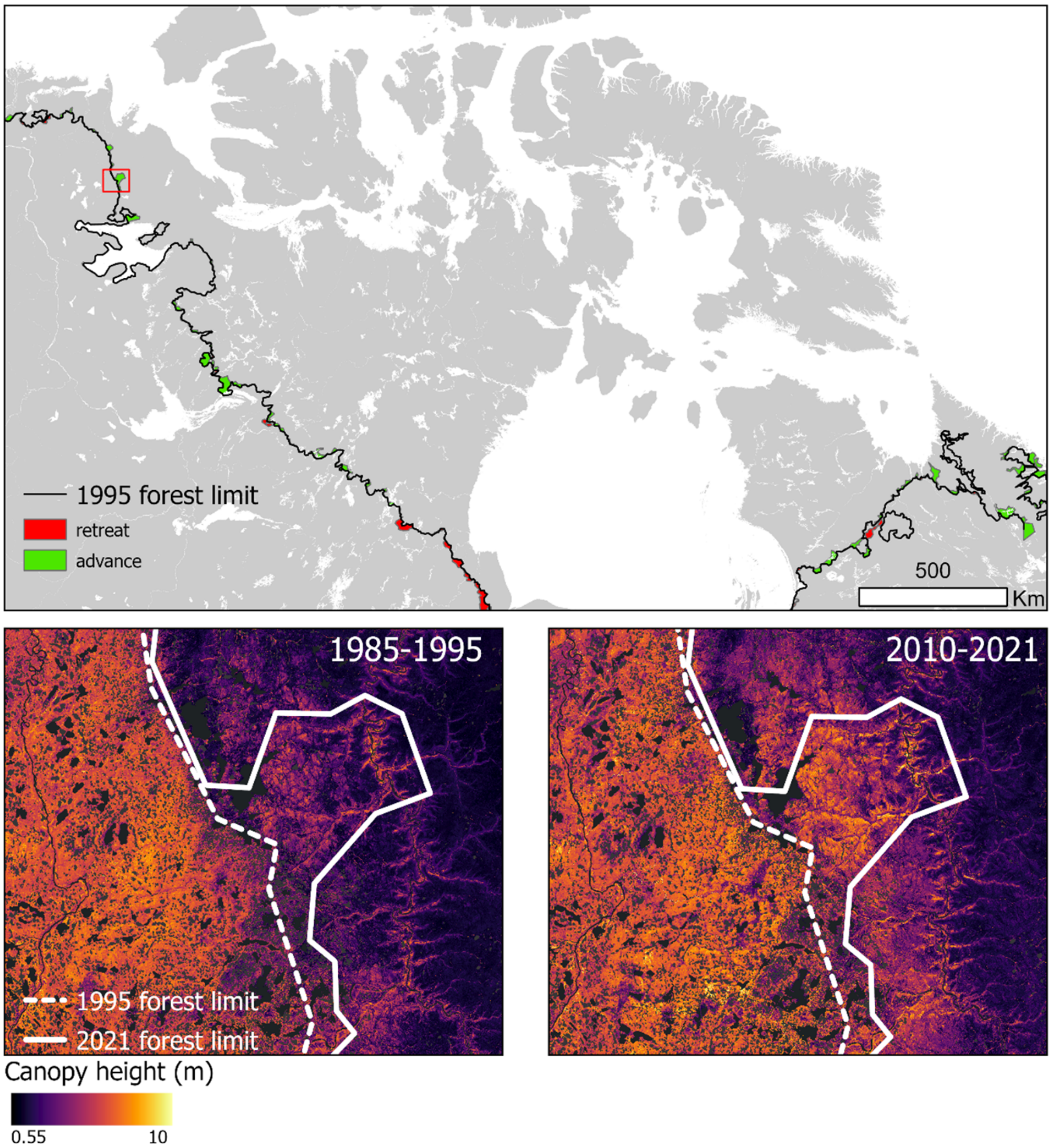

Figure 3. Mapping retreat and advance of the northern limit of continuous 3 m forest using canopy height and presence in the 1985–1995 and 2010–2021 time periods. The inset map highlights a region where the forest limit has advanced northward. The canopy height data is mapped at 30 m spatial resolution.

4. Discussion

In this study, we used spaceborne lidar and spectral-time series data to map change in vegetation structure across the Canadian FTE over a 36 year period. Our results support mapping conducted with high-resolution air photos showing limited treeline advance across North America, despite increases in temperature and precipitation (Lantz *et al* 2019, Timoney and Mamet 2020, Travers-Smith and Lantz 2020, Maher *et al* 2021). We show overall stability in the cover of shrub (1–3 m) and forest (>3 m) canopies across the ecotone. However, the distribution of "new shrub" and "new forest" classes diverged patterns across the forest limit. Forest expansion was concentrated below the historic forest limit, while shrub expansion was more frequent above the forest limit. These findings are also consistent with analysis of forest cover change in Canada by Hermosilla *et al* (2025), who reported infilling of trees in proximity to existing treed areas and recovery from wildfires predating the Landsat record in the mid-1980's. The strong association between vegetation change types and the timing of fires also indicates that current and future fire regimes will play significant role in vegetation dynamics over decadal time scales.

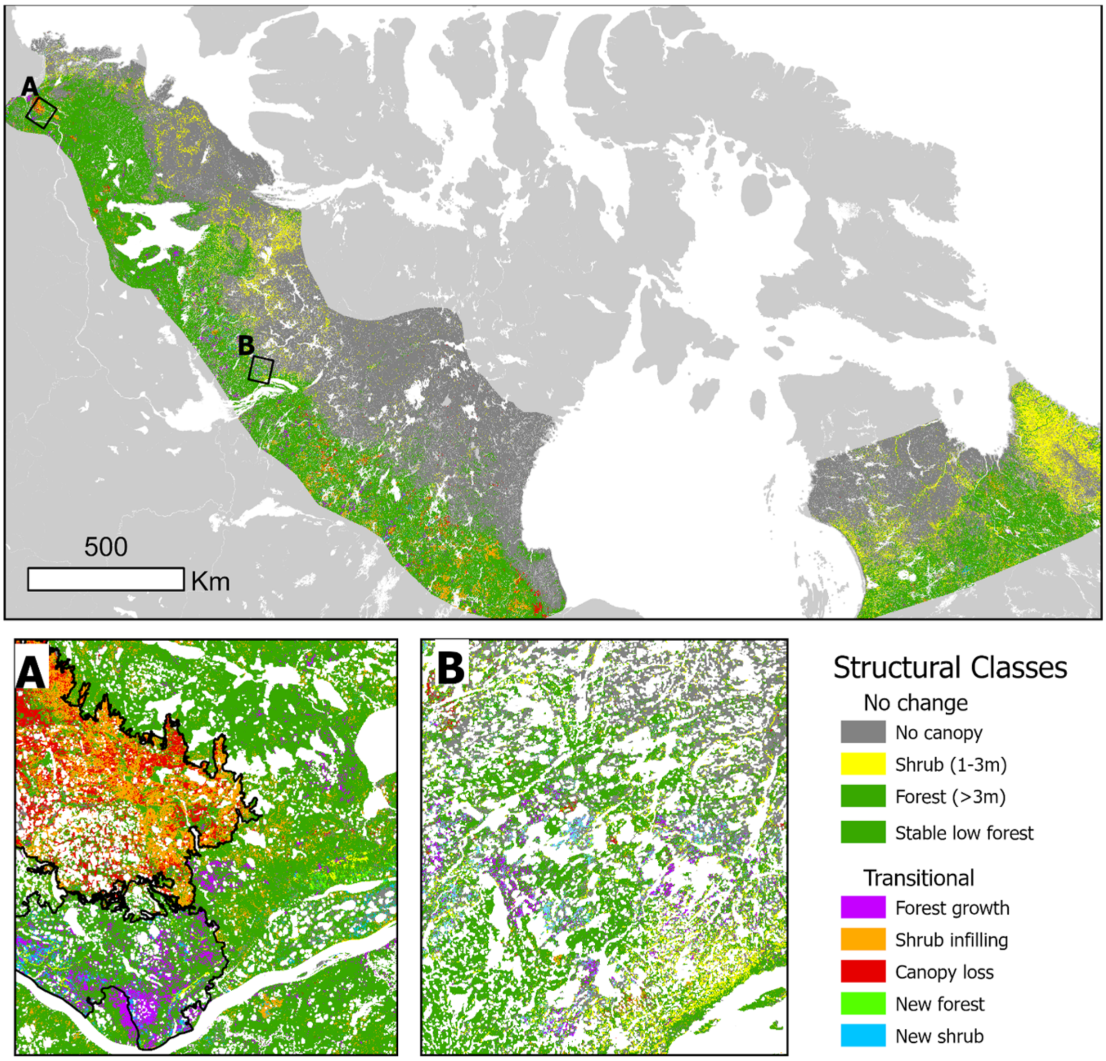

Figure 4. Map of structural vegetation classes across the study area. The inset maps show detail in the 30 m change product. Panel A also highlights structural change within the extent of two fires that burned in 1999 and 1968 (black outline). Water and unclassified pixels areas are shown in white.

Table 2. Summary table showing the proportion of structural vegetation change across the entire study area and stratified by ecoregion (%). The bold text shows the total proportion of stable and transitional classes and the proportional coverage of each ecoregion over the entire study area.

Structural class	Taiga Plains	Taiga Shield	Southern Arctic	Arctic Cordillera	Hudson Plains	Overall
Stable no canopy	10.0	33.2	80.3	19.8	56.5	45.4
Stable shrub (1–3 m)	0.8	9.5	7.3	59.2	0.6	9.0
Stable forest (>3 m)	74.3	43.5	8.6	12.9	31.6	34.9
Stable low forest	3.2	3.1	1.5	4.6	3.5	2.7
Total Stable	**88.3**	**89.3**	**97.7**	**96.6**	**92.2**	**92.1**
Forest growth	4.5	2.3	0.3	0.6	0.5	1.8
Shrub infilling	4.7	4.8	0.2	0.4	1.5	3.2
Canopy loss	1.5	1.5	0.6	0.5	4.8	1.2
New forest	0.8	1.0	0.2	0.6	0.4	0.7
New shrub	0.2	1.1	1.0	1.2	0.6	0.9
Total Transitional	**11.7**	**10.7**	**2.3**	**3.3**	**7.8**	**7.8**
Ecozone % of total	**10.0%**	**55.1%**	**30.4%**	**2.5%**	**1.6%**	—

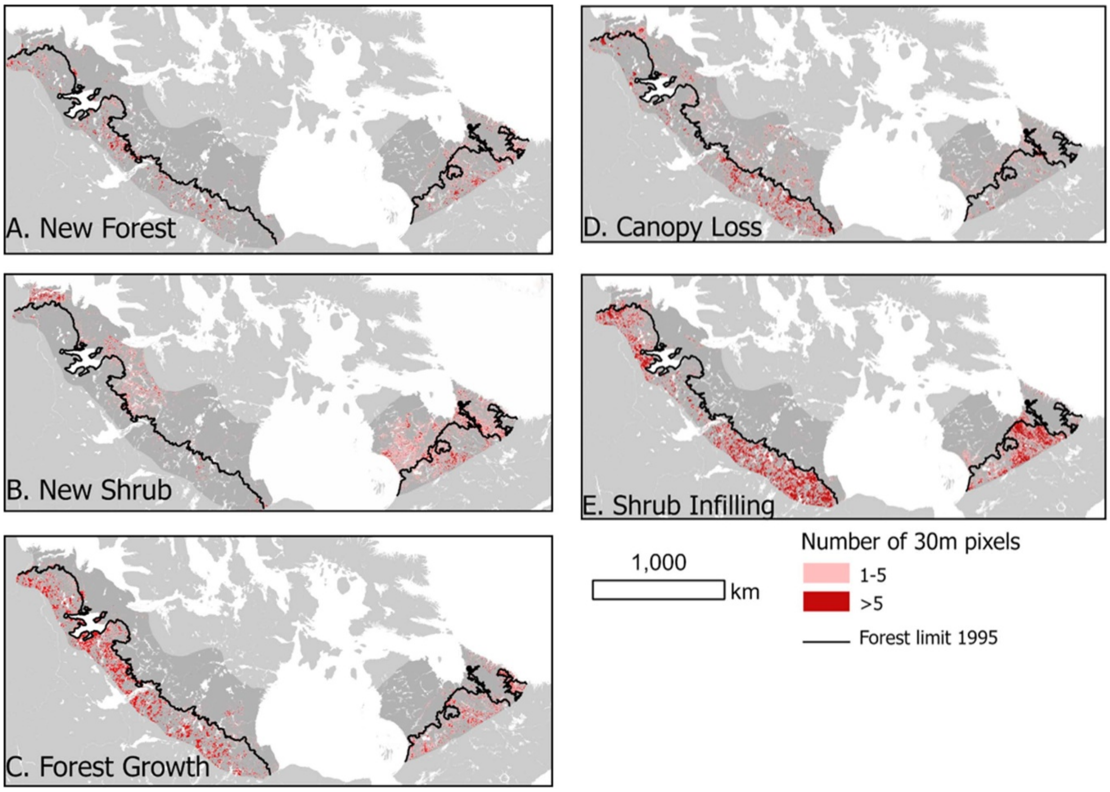

Figure 5. Distribution of transitional vegetation classes across the study area relative to the 1995 forest limit. For visualization, 30 m pixels were aggregated into 300 × 300 m cells and the number of pixels of each class were counted per cell.

Table 3. Summary table showing the proportion of vegetation classes stratified by disturbance history within the Northwest Territories (%).

Structural class	Undisturbed	Burned 1950–1985	Burned 1985–1999	Burned 2000–2011
Stable no canopy	52.3	7.2	8.0	4.4
Stable shrub (1–3 m)	4.9	4.4	1.4	1.1
Stable forest (>3 m)	34.4	58.9	59.6	63.1
Stable low forest	1.9	4.5	6.8	1.9
Total stable	**93.5**	**75.0**	**75.8**	**70.5**
Forest growth	1.9	17.3	0.7	0.2
Shrub infilling	2.6	0.5	14.2	23.6
Canopy loss	1.0	0.2	8.0	5.5
New forest	0.4	6.1	0.6	0.1
New shrub	0.5	0.9	0.7	0.1
Total transitional	**6.4**	**25.0**	**24.2**	**29.4**
% of total	**88.2**	**4.6**	**1.4**	**2.5**

4.1. Remotely sensed models of vegetation structure

Our results highlight the importance of multiple spectral indices for understanding vegetation change in the FTE. Longer wavelengths including the SWIR2 band, and the TCB index which integrates reflectance across all spectral bands were significant predictors of canopy presence and height. Overall, tall-stature vegetation was characterized by low brightness and lower NIR and SWIR reflectance, likely driven by the density of coniferous trees (Olthof and Fraser 2007). Conifers have a high proportion of dark woody material and foliage that casts shadows that can decrease surface reflectance within medium spatial resolution pixels (Cohen and Spies 1992, Pickell *et al* 2016). In contrast, low-stature vegetation (<3 m) was characterized by higher NIR reflectance and TCG values (figure 3), likely driven by greater phytomass and Leaf Area Index of tall deciduous shrubs (Walker *et al* 2003, McManus *et al* 2012).

ICESat-2 provides measurements of vegetation structure across the entire circumpolar Arctic that can support mapping at broad spatial scales (Sothe *et al* 2022, Lang *et al* 2023). However, several studies show that ICESat-2 can overestimate the height of low-stature vegetation which can propagate in models of vegetation height (Neuenschwander and Pitts 2019, Feng et al 2023). In this study we focus on identifying change over time which mitigates potential biases in overestimating low canopy heights. Future work focusing on growth of tundra shrubs should incorporate higher resolution lidar data available at regional scales. This includes airborne lidar data from the LVIS instrument in Alaska and north-western Canada (Blair and Hofton 2020), and the growing availability of photogrammetric data from drones (Cunliffe et al 2022, van der Sluijs et al 2023). The spatial resolution of our mapping (30 m) also limits our ability to detect recent establishment of northern spruce seedlings which may take up to 75 years to reach a height and density visible in satellite imagery (Timoney 2023). Furthermore, using spaceborne lidar we are only able to detect upright tree growth forms rather than matted or 'whorled' structures which are common for black spruce at the northern treeline (Lavoie and Payette 1992). Higher-resolution mapping and long-term monitoring plots are needed to understand these subtle vegetation changes and determine if shifts in the position of the treeline will occur over centuries or decades.

4.2. Structural vegetation dynamics

Meta-analyses of global treelines have suggested that the majority of treelines have advanced in elevation or latitude (Harsch et al 2009, Hansson et al 2021). However, sites representing latitudinal treelines comprise only 8%–24% of these datasets, indicating that they are under sampled globally. We observed limited evidence of systemic forest advance, despite increases in mean annual temperature and total precipitation at the forest limit. Our mapping reveals local areas of both advance and retreat in the boundary of continuous forest, but highlights overall stability of this boundary. This is consistent with several studies using field-data and high-resolution mapping conducted across the Northwest Territories (Lantz et al 2019, Travers-Smith and Lantz 2020), Nunavut (MacDonald et al 1998, Timoney and Mamet 2020, Timoney 2023) and northern Quebec (Gamache and Payette 2004, 2005) documenting limitations in tree recruitment and range expansion beyond the northern treeline. In black spruce forest across the Taiga Shield, edaphic factors including nutrient-poor and shallow soils underlain by bedrock can restrict expansion of the boreal forest even with favorable climate conditions (Timoney 2023).

Disturbance history shows that older fires that burned prior to 1985 were primary divers of increasing vegetation structure. Compared to undisturbed regions fires had higher proportions of 'forest growth', 'new forest' and 'new shrub' transitions. This follows with previous analysis of greening trends in the Canadian boreal, which were concentrated and magnified in disturbed rather than undisturbed areas (Sulla-Menashe et al 2018). These findings indicate that climate driven increases in vegetation structure are relatively small in comparison to disturbance-recovery processes. As expected, recent fires were more likely to show decreases in vegetation structure. This also reflects the time required for tall-stature vegetation to establish and reach densities sufficient to be detected in medium resolution satellite data (Timoney et al 2019). However, this could also indicate more persistent shifts in vegetation communities as upright shrubs can also exhibit long-term increases in cover following fire (Lantz et al 2010, Gaglioti et al 2021, Miller et al 2024).

5. Conclusion

We used satellite remote-sensing to map multiple types of structural vegetation change in 183 million ha of the Canadian FTE between 1985 and 2021. Forest and shrub range expansion showed divergent patterns across the ecotone, with a greater proportion of shrub expansion occurring above the historic forest limit. The northern forest limit showed localized expansion representing ~15 000 km^2 (0.9%) of new forested area, but large parts remained stable over the past 40 years. We show that the forest limit has also experienced increases in mean annual temperature and precipitation, suggesting weaker associations between decadal climate change and northward forest advance. Our findings show that increasing vegetation structure was strongly associated with fire history, highlighting the importance of disturbance-recovery dynamics in future vegetation change. Future work should use novel sources of high-resolution imagery, airborne lidar data and field data to improve confidence in models of vegetation change across the circumpolar.

Data availability statement

Open access code and sample datasets supporting this work can be found in the following repository: Travers-Smith (2024), 'Replication Data for: Satellite observations reveal stable forest limits and shrub expansion across the Canadian forest-tundra ecotone' at https://doi.org/10.5683/SP3/JZW3H2. Additional model outputs and code are available at request from the authors.

Acknowledgment

This research was funded in part through the Canadian Space Agency (Grant number: 21SUESECDL). We also acknowledge funding support to Hana Travers-Smith from the NSERC Canada Graduate Scholarship-Doctoral and the University of British Columbia.

Author contributions

H Travers-Smith
Conceptualization (lead), Formal analysis (lead), Investigation (lead), Methodology (lead), Visualization (lead), Writing – original draft (lead)

N C Coops
Conceptualization (equal), Funding acquisition (equal), Project administration (equal), Supervision (equal), Writing – review & editing (equal)

C Mulverhill
Methodology (equal), Writing – review & editing (equal)

M A Wulder 0000-0002-6942-1896
Supervision (equal), Writing – review & editing (equal)

T C Lantz
Supervision (equal), Writing – review & editing (equal)

D D Ignace
Supervision (equal), Writing – review & editing (equal)

References

Arndt K A, Santos M J, Ustin S, Davidson S J, Stow D, Oechel W C, Tran T T P, Graybill B and Zona D 2019 Arctic greening associated with lengthening growing seasons in Northern Alaska *Environ. Res. Lett.* **14** 125018

Berner L T *et al* 2020 Summer warming explains widespread but not uniform greening in the Arctic tundra biome *Nat. Commun.* **11** 4621

Berner L T and Goetz S J 2021 Satellite observations document trends consistent with a boreal forest biome shift *Glob. Change Biol.* **28** 3275–92

Blair J B and Hofton M 2020 *LVIS Facility L2 Geolocated Surface Elevation and Canopy Height Product, Version 1* (NASA National Snow and Ice Data Center Distributed Active Archive Center) (https://doi.org/10.5067/VP7J20HJQISD)

Bolton D K, White J C, Wulder M A, Coops N C, Hermosilla T and Yuan X 2018 Updating stand-level forest inventories using airborne laser scanning and Landsat time series data *Int. J. Appl. Earth Obs. Geoinf.* **66** 174–83

Box J E *et al* 2019 Key indicators of Arctic climate change: 1971–2017 *Environ. Res. Lett.* **14** 045010

Brodie J F, Roland C A, Stehn S E and Smirnova E 2019 Variability in the expansion of trees and shrubs in boreal Alaska *Ecology* **100** e02660

Chapin F S III *et al* 2000 Arctic and boreal ecosystems of western North America as components of the climate system *Glob. Change Biol.* **6** 211–23

Chen A, Lantz T C, Hermosilla T and Wulder M A 2021 Biophysical controls of increased tundra productivity in the western Canadian Arctic *Remote Sens. Environ.* **258** 112358

Cohen W B and Spies T A 1992 Estimating structural attributes of Douglas-fir/western hemlock forest stands from Landsat and SPOT imagery *Remote Sens. Environ.* **41** 1–17

Cunliffe A M *et al* 2022 Global application of an unoccupied aerial vehicle photogrammetry protocol for predicting aboveground biomass in non-forest ecosystems *Remote Sens. Ecol. Conserv.* **8** 57–71

Ecosystem Classification Group 2007 *Ecological Regions of the Northwest Territories—Taiga Plains* (p. viii + 173 pp. + insert map) (Department of Environment and Natural Resources, Government of the Northwest Territories) (available at: www.gov.nt.ca/ecc/sites/ecc/files/resources/taiga_plains_ecological_land_classification_report.pdf)

Ecosystem Classification Group 2008 *Ecological Regions of the Northwest Territories—Taiga Shield* (p. viii + 146 pp. + insert map) (Department of Environment and Natural Resources, Government of the Northwest Territories) (available at: www.enr.gov.nt.ca/sites/enr/files/resources/taiga_shield_ecological_land_classification_report_0.pdf)

Ecosystem Classification Group 2012 *Ecological Regions of the Northwest Territories—Southern Arctic* (No. x + 170 pp. + insert map) (Department of Environment and Natural Resources, Government of the Northwest Territories)

Epstein H E, Raynolds M K, Walker D A, Bhatt U S, Tucker C J and Pinzon J E 2012 Dynamics of aboveground phytomass of the circumpolar Arctic tundra during the past three decades *Environ. Res. Lett.* **7** 015506

Evans P and Brown C D 2017 The boreal–temperate forest ecotone response to climate change *Environ. Rev.* **25** 423–31

Feng T, Duncanson L, Montesano P, Hancock S, Minor D, Guenther E and Neuenschwander A 2023 A systematic evaluation of multi-resolution ICESat-2 ATL08 terrain and canopy heights in boreal forests *Remote Sens. Environ.* **291** 113570

Fraser R H, Van der Sluijs J and Hall R J 2017 Calibrating satellite-based indices of burn severity from UAV-derived metrics of a burned boreal forest in NWT, Canada *Remote Sens.* **9** 279

Gaglioti B V, Berner L T, Jones B M, Orndahl K M, Williams A P, Andreu-Hayles L, D'Arrigo R D, Goetz S J and Mann D H 2021 Tussocks enduring or shrubs greening: alternate responses to changing fire regimes in the Noatak River Valley, Alaska *J. Geophys. Res.* **126** e2020JG006009

Gamache I and Payette S 2004 Height Growth response of tree line black spruce to recent climate warming across the forest-tundra of Eastern Canada *J. Ecol.* **92** 835–45

Gamache I and Payette S 2005 Latitudinal response of subarctic tree lines to recent climate change in eastern Canada *J. Biogeograph.* **32** 849–62

Guay K C, Beck P S A, Berner L T, Goetz S J, Baccini A and Buermann W 2014 Vegetation productivity patterns at high northern latitudes: a multi-sensor satellite data assessment *Glob. Change Biol.* **20** 3147–58

Hansson A, Dargusch P and Shulmeister J 2021 A review of modern treeline migration, the factors controlling it and the implications for carbon storage *J. Mount. Sci.* **18** 291–306

Harsch M A, Hulme P E, McGlone M S and Duncan R P 2009 Are treelines advancing? A global meta-analysis of treeline response to climate warming *Ecol. Lett.* **12** 1040–9

Hermosilla T, Wulder M A, White J C, Bater C W, Baral S K and Leach J A 2025 Expansion of treed area over Canada's forested ecosystems: spatial and temporal trends *Forestry* **1** cpaf015

Hermosilla T, Wulder M A, White J C and Coops N C 2022 Land cover classification in an era of big and open data: optimizing localized implementation and training data selection to improve mapping outcomes *Remote Sens. Environ.* **268** 112780

Hermosilla T, Wulder M A, White J C, Coops N C and Hobart G W 2015 An integrated Landsat time series protocol for change detection and generation of annual gap-free surface reflectance composites *Remote Sens. Environ.* **158** 220–34

Hermosilla T, Wulder M A, White J C, Coops N C and Hobart G W 2018 Disturbance-informed annual land cover classification maps of Canada's forested ecosystems for a 29-year landsat time series *Can. J. Remote Sens.* **44** 67–87

Hermosilla T, Wulder M A, White J C, Coops N C, Hobart G W and Campbell L B 2016 Mass data processing of time series

Landsat imagery: pixels to data products for forest monitoring *Int. J. Digit. Earth* **9** 1035–54
Hijmans R J 2022 Raster: geographic data analysis and modeling (available at: https://CRAN.R-project.org/package=raster)
Lang N, Jetz W, Schindler K and Wegner J D 2023 A high-resolution canopy height model of the Earth *Nat. Ecol. Evol.* **7** 1778–89
Lantz T C, Gergel S E and Henry G H R 2010 Response of green alder (Alnus viridis subsp. Fruticosa) patch dynamics and plant community composition to fire and regional temperature in north-western Canada *J. Biogeograph.* **37** 1597–610
Lantz T C, Moffat N D, Fraser R H and Walker X 2019 Reproductive limitation mediates the response of white spruce (*Picea glauca*) to climate warming across the forest–tundra ecotone *Arct. Sci.* **5** 167–84
Lavoie C and Payette S 1992 Black spruce growth forms as a record of a changing winter environment at Treeline, Quebec, Canada *Arct. Alp. Res.* **24** 40–49
Loranty M, Davydov S P, Kropp H, Alexander H D, Mack M C, Natali S M and Zimov N S 2018 Vegetation indices do not capture forest cover variation in upland Siberian larch forests *Remote Sens.* **10** 1686
MacDonald G M, Szeicz J M, Claricoates J and Dale K A 1998 Response of the central Canadian treeline to recent climatic changes *Ann. Assoc. Am. Geogr.* **88** 183–208
Magruder L, Brunt K, Neumann T, Klotz B and Alonzo M 2021 Passive ground-based optical techniques for monitoring the on-orbit ICESat-2 altimeter geolocation and footprint diameter *Earth Space Sci.* **8** e2020EA001414
Maher C T, Dial R J, Pastick N J, Hewitt R E, Jorgenson M T and Sullivan P F 2021 The climate envelope of Alaska's northern treelines: implications for controlling factors and future treeline advance *Ecography* **44** 1710–22
Malambo L, Popescu S and Liu M 2023 Landsat-scale regional forest canopy height mapping using ICESat-2 along-track heights: case study of eastern texas *Remote Sens.* **15** 1
Margolis H A, Nelson R F, Montesano P M, Beaudoin A, Sun G, Andersen H-E and Wulder M A 2015 Combining satellite lidar, airborne lidar, and ground plots to estimate the amount and distribution of aboveground biomass in the boreal forest of North America *Can. J. For. Res.* **45** 838–55
Markus T *et al* 2017 The ice, cloud, and land elevation Satellite-2 (ICESat-2): science requirements, concept, and implementation *Remote Sens. Environ.* **190** 260–73
Matasci G, Hermosilla T, Wulder M A, White J C, Coops N C, Hobart G W, Bolton D K, Tompalski P and Bater C W 2018 Three decades of forest structural dynamics over Canada's forested ecosystems using Landsat time-series and lidar plots *Remote Sens. Environ.* **216** 697–714
McManus K M, Morton D C, Masek J G, Wang D, Sexton J O, Nagol J R, Ropars P and Boudreau S 2012 Satellite-based evidence for shrub and graminoid tundra expansion in northern Quebec from 1986 to 2010 *Glob. Change Biol.* **18** 2313–23
Miller E A, Baughman C A, Jones B M and Jandt R R 2024 Biophysical effects of an old tundra fire in the Brooks Range Foothills of Northern Alaska, U.S.A *Polar Sci.* **39** 100984
Mishra N, Helder D, Barsi J and Markham B 2016 Continuous calibration improvement in solar reflective bands: Landsat 5 through Landsat 8 *Remote Sens. Environ.* **185** 7–15
Montesano P M, Frost M, Li J, Carroll M, Neigh C S R, Macander M J, Sexton J O and Frost G V 2024 A shift in transitional forests of the North American boreal will persist through 2100 *Commun. Earth Environ.* **5** 1–10
Mulverhill C, Coops N C, Hermosilla T, White J C and Wulder M A 2022 Evaluating ICESat-2 for monitoring, modeling, and update of large area forest canopy height products *Remote Sens. Environ.* **271** 112919
Myers-Smith I H *et al* 2011 Shrub expansion in tundra ecosystems: dynamics, impacts and research priorities *Environ. Res. Lett.* **6** 045509
Myers-Smith I H *et al* 2020 Complexity revealed in the greening of the Arctic *Nat. Clim. Change* **10** 106–17
Neuenschwander A, Guenther E, White J C, Duncanson L and Montesano P 2020 Validation of ICESat-2 terrain and canopy heights in boreal forests *Remote Sens. Environ.* **251** 112110
Neuenschwander A and Pitts K 2019 The ATL08 land and vegetation product for the ICESat-2 Mission *Remote Sens. Environ.* **221** 247–59
NWT Centre for Geomatics 2024 Fire history (available at: www.geomatics.gov.nt.ca/en/fire-history)
Olthof I and Fraser R H 2007 Mapping northern land cover fractions using Landsat ETM+ *Remote Sens. Environ.* **107** 496–509
Orndahl K M, Macander M J, Berner L T and Goetz S 2022 Plant functional type aboveground biomass change within Alaska and northwest Canada mapped using a 35-year satellite time series from 1985–2020 *Environ. Res. Lett.* **17** 115010
Payette S, Fortin M-J and Gamache I 2001 The subarctic forest–tundra: the structure of a biome in a changing climate: the shifting of local subarctic tree lines throughout the forest–tundra biome, which is linked to ecological processes at different spatiotemporal scales, will reflect future global changes in climate *BioScience* **51** 709–18
Pearson R G, Phillips S J, Loranty M M, Beck P S A, Damoulas T, Knight S J and Goetz S J 2013 Shifts in Arctic vegetation and associated feedbacks under climate change *Nat. Clim. Change* **3** 673–7
Pickell P D, Hermosilla T, Frazier R J, Coops N C and Wulder M A 2016 Forest recovery trends derived from Landsat time series for North American boreal forests *Int. J. Remote Sens.* **37** 138–49
Rickbeil G J M, Hermosilla T, Coops N C, White J C, Wulder M A and Lantz T C 2018 Changing northern vegetation conditions are influencing barren ground caribou (Rangifer tarandus groenlandicus) post-calving movement rates *J. Biogeograph.* **45** 702–12
Rotbarth R, Van Nes E H, Scheffer M, Jepsen J U, Vindstad O P L, Xu C and Holmgren M 2023 Northern expansion is not compensating for southern declines in North American boreal forests *Nat. Commun.* **14** 3373
Royal Canadian Geographical Society 2018a *Canadian Geographic Indigenous Peoples Atlas of Canada: Inuit: Vol. Inuit* (The Royal Canadian Geographical Society)
Royal Canadian Geographical Society 2018b *Canadian Geographic Indigenous Peoples Atlas of Canada: Vol. Indigenous Canada* (The Royal Canadian Geographical Society)
Shah S A A, Manzoor M A and Bais A 2020 Canopy height estimation at Landsat resolution using convolutional neural networks *Mach. Learn. Knowl. Extraction* **2** 23–36
Sothe C, Gonsamo A, Lourenço R B, Kurz W A and Snider J 2022 Spatially continuous mapping of forest canopy height in Canada by combining GEDI and ICESat-2 with PALSAR and sentinel *Remote Sens.* **14** 5158
Speed J D M, Chimal-Ballesteros J A, Martin M D, Barrio I C, Vuorinen K E M and Soininen E M 2021 Will borealization of Arctic tundra herbivore communities be driven by climate warming or vegetation change? *Glob. Change Biol.* **27** 6568–77
Sulla-Menashe D, Friedl M A and Woodcock C E 2016 Sources of bias and variability in long-term Landsat time series over Canadian boreal forests *Remote Sens. Environ.* **177** 206–19
Sulla-Menashe D, Woodcock C E and Friedl M A 2018 Canadian boreal forest greening and browning trends: an analysis of biogeographic patterns and the relative roles of disturbance versus climate drivers *Environ. Res. Lett.* **13** 014007
Tachikawa T *et al* 2011 *ASTER Global Digital Elevation Model Version 2—Summary of Validation Results* (NASA)
Terskaia A, Dial R J and Sullivan P F 2020 Pathways of tundra encroachment by trees and tall shrubs in the western Brooks Range of Alaska *Ecography* **43** 769–78

Timoney K P 2023 No evidence of a northward biome shift of treeline in the Mackay Lake region, north-central Canada *Écoscience* **30** 113–29

Timoney K P, La Roi G H, Zoltai S C and Robinson A L 1992 The high subarctic forest-tundra of northwestern Canada: position, width, and vegetation gradients in relation to climate *ARCTIC* **45** 1–9

Timoney K P, Mamet S D, Cheng R, Lee P, Robinson A L, Downing D and Wein R W 2019 Tree cover response to climate change in the forest-tundra of north-central Canada: fire-driven decline, not northward advance *Écoscience* **26** 133–48

Timoney K P and Mamet S 2020 No treeline advance over the last 50 years in subarctic western and central Canada and the problem of vegetation misclassification in remotely sensed data *Écoscience* **27** 93–106

Travers-Smith H Z and Lantz T C 2020 Leading-edge disequilibrium in alder and spruce populations across the forest–tundra ecotone *Ecosphere* **11** e03118

Travers-Smith H, Coops N C, Lantz T C, Hamp M, Ignace D, Wulder M A and Van Der Sluijs J 2025 Vegetation structure and soil organic carbon storage across northern forest-tundra ecotones in continuous permafrost *Arct. Sci.* **11** 1–18

Travers-Smith H, Coops N C, Mulverhill C, Wulder M A, Ignace D and Lantz T C 2024 Mapping vegetation height and identifying the northern forest limit across Canada using ICESat-2, Landsat time series and topographic data *Remote Sens. Environ.* **305** 114097

van der Sluijs J, Saiet E, Bakelaar C N, Wentworth A, Fraser R H and Kokelj S V 2023 Beyond visual-line-of-sight (BVLOS) drone operations for environmental and infrastructure monitoring: a case study in northwestern Canada *Drone Syst. Appl.* **11** 1–15

Vincent L A, Hartwell M M and Wang X L 2020 A third generation of homogenized temperature for trend analysis and monitoring changes in Canada's climate *Atmosphere* **58** 173–91

Walker D A *et al* 2003 Phytomass, LAI, and NDVI in northern Alaska: relationships to summer warmth, soil pH, plant functional types, and extrapolation to the circumpolar Arctic *J. Geophys. Res. Atmos.* **108**

Walker X J, Alexander H D, Berner L T, Boyd M A, Loranty M M, Natali S M and Mack M C 2021 Positive response of tree productivity to warming is reversed by increased tree density at the Arctic tundra–taiga ecotone *Can. J. For. Res.* **51** 1323–38

Wang T, Hamann A, Spittlehouse D and Carroll C 2016 Locally downscaled and spatially customizable climate data for historical and future periods for North America *PLoS One* **11** e0156720

White J C *et al* 2014 Pixel-based image compositing for large-area dense time series applications and science *Can. J. Remote Sens.* **40** 192–212

Wright M N and Ziegler A 2017 Ranger: a fast implementation of random forests for high dimensional data in C++ and R *J. Stat. Softw.* **77** 1–17